Journal of Applied Fluid Mechanics, Vol. 6, No. 9, pp. 1729-1741, 2023.
Available online at www.jafmonline.net, ISSN 1735-3572, EISSN 1735-3645.
https://doi.org/10.47176/jafm.16.09.1805

Experimental and Numerical Dynamic Investigation of a Swirling Jet: Application to Improve the Efficiency of Air Diffusion in an Occupied Zone

A. Bennia[1,2,†], A. Reffas[1], M. A. H. Khan[2], H. E. Mohamadi[3], M. Lateb[4] and H. Fellouah[4]

[1]*Department of Electromechanics, University Mohamed El Bachir El Ibrahimi of Bordj Bou Arreridj, El-Anasser, 34030 Algeria*
[2]*Control, Testing, Measurement and Mechanical Simulation Laboratory, University Hassiba Benbouali Hay Salem, National Road 19, Chlef, 02000 Algeria*
[3] *Department of Software and IT Engineering, École de technologie supérieure, Rue Notre-Dame Ouest, Montréal, Qc, H3C 1K3 Canada*
[4]*Department of Mechanical Engineering, Université de Sherbrooke 2500 Blvd. de l'Université, Sherbrooke Qc, J1K 2R1 Canada*

†*Corresponding Author Email:Abderazak.Bennia@usherbrooke.ca*

ABSTRACT

When reducing the energy prerequisites of buildings, the correct distribution of fresh air flows injected into the living rooms poses a problem. If the problem of mixing the injected air in the ambient air is not effectively solved, there will be a strong deterioration in air quality and comfort. In this research, a new design of swirling diffuser is investigated experimentally and numerically using large eddy simulations. The influence of fins is studied for the improvement of air diffusion and jet mixing with ambient air. The study was carried out for a fins angle of 30° with the jet's axis and 60° with the blowing orifice's plane with the condition of uniform heat flux of the air. The working fluid used is air. It has been validated that using fins leads to a greater spreading of the jet and good air mixing compared to those obtained from smooth tubes (circular nozzle). To enhance the accuracy of the turbulence models' predictions, three turbulence models are tested: the wall-adapting local eddy-viscosity turbulence model (LES/WALEVM), Smagorinski-Lilly (LES/S-LM) model and the kinetic-energy transport model (LES/K-ETM). It is worth highlighting that the LES/K-ETM model is well established in the prediction of swirling flows, which have been successfully compared with experimental results.

Article History

Received February 6, 2023
Revised April 18, 2023
Accepted April 29, 2023
Available online July 1, 2023

Keywords:

Swirl diffusers
Large eddy simulation
Indoor air quality
CFD
Turbulence models

1. INTRODUCTION

Swirl diffusers are increasingly gaining momentum by researchers because of their low energy consumption and high diffusion efficiency. Over the past decade, researchers have conducted both experimental and numerical investigations on the swirling nozzle performance, which have resulted in significant insights into their diffusion efficiency, flow structures, and geometrical characteristics. Moreover, the application of CFD methods has recently increased to analyze indoor airflows and determine how various design factors affect indoor air quality.

As such, swirling jet is a modern type of air jet that can ensure better mixing through the generation of air vortexes and enhance the Coanda effect by using centrifugal force (Nielsen, 1992). Extensive study has been conducted, both experimentally and numerically, to examine the effect of different parameters on the flow development behind the fins of a swirl generator. The following section provides a brief review of some of the notable research achievements in this area. The best approach for analyzing the airflows produced by swirl diffusers is through experimentation. Despite the importance of analyzing the airflows produced by swirl diffusers, there is a lack of experimental studies due to the challenges involved in accurately measuring flow fields (Hu, 2003; Aziz et al., 2012; Raftery et al., 2015). To examine the airflow patterns of swirl diffusers, most of the pertinent experimental research (Aziz et al., 2012; Raftery et al,. 2015) used spatially localized data.

Despite the potential benefits of using swirling jets to improve comfort conditions, there has been limited research on this application. Swirling jets are commonly used in diverse industrial techniques, such as cooling electronic parts or gas turbine blades, to optimize heat

Nomenclature

D_e	equivalent diameter	μ_t	subgrid-scale eddy viscosity
r/D_e	radial direction (dimensionless radius)	R_{ij}	Reynolds stress-like term
x/D_e	axial direction (dimensionless height)	κ	Von Kármán's constant
α_a	fins' angles with the jet axis	C_s	Smagorinsky's constant
α_b	fins' angles with the plane of blow	d	distance to nearest wall
τ_{ij}	subgrid stress tensor	C_{ij}	Clark tensor
$\bar{S}_{ij}$	rate-of-strain tensor	V	volume of the computational cell
L_s	mixing length for subgrid scales	λ	thermal conductivity
h_s	sensible enthalpy	Δ	local grid scale
λ	thermal conductivity	LES	Large-Eddy Simulation
μ_t	subgrid-scale eddy viscosity	LES/WALEVM	Wall-Adapting Local Eddy Viscosity turbulence model
L_{ij}	Leonard tensor	LES/S-LM	Smagorinsky-Lilly model
U_r	reduced velocities	LES/K-ETM	Kinetic-Energy Transport model
L_s	mixing length for subgrid scales	HVAC	Heating, Ventilation and Air Conditioning
h_s	sensible enthalpy	CFD	Computational Fluid Dynamics

transfer. Most research on swirling jets under various conditions aims to improve combustion by enhancing the mixing between the oxidizer and the fuel. (Kumar et al., 2022; Wang et al,. 2022; Xie et al., 2022). Experimental and numerical studies published by Bennia et al. (2015, 2016, 2018, 2020) have demonstrated the potential for improving air diffusion in residential premises by implementing turbulent jets.

In this context, a numerical approach enabling full information on the flow fields is CFD. One of the first researchers to use CFD techniques to forecast heat transfer and air flow in buildings was Nielsen (Nielsen, 1976, 2015). Without a doubt, the prediction of indoor airflow by CFD has advanced HVAC system design (Awbi, 1989; Huo et al,. 2000; Zhao et al., 2003; Luo et al., 2004; Nielsen, 2015; Khan et al., 2022). Based on the turbulence models, the current computational methods for studying swirl diffusers may be loosely divided into two groups: (i) LES models (Tavakoli & Hosseini 2013) and (ii) RANS models (Aziz et al., 2012; Villafruela et al,. 2013; Yau et al., 2018).

It is widely known that among the most significant factors that may determine the characteristics of indoor airflow is the shape of the air diffuser. (Nielsen, 1992). Due to the complex geometries of most diffusers and the large disparity in size between them and the room, performing numerical modeling of air flow from diffusers can be challenging. This difference creates a significant skewness or high mesh aspect ratio in the region close to the diffuser, which not only leads to convergence problems but also has an impact on the precision of the findings. Accordingly, numerous research projects have been done to give the correct models that describe as closely as possible the air flow of supply diffusers. There are at least four different methods that can be used to model airflow from diffusers: basic models (Nielsen, 1989), momentum models (Koskela, 2004), box models (Nielsen, 1997), and prescribed velocity models (Nielsen, 1998). In a single study in this field, Hu (2003) analyzed the airflow characteristics in a particular type of swirling diffuser with complex design. To do so, he used a hybrid zonal mesh of tetrahedral and hexahedral elements and found that the predicted results were consistent with the experimental ones. However, Hu (2003) did not investigate how the fins geometry could affect the performance of the diffuser, which appears to be one of the most important parameters.

Airflow through swirling diffusers is studied numerically by Sajadi et al. (2011). A parametric analysis is used to assess how the primary geometric characteristics affect the induction effect and the Efficiency of the diffuser. The results help to improve understanding the impact of diffuser design on the resulting airflow and the effect of induction.

This paper proposes a new design for a swirling diffuser and presents the research conducted on its diffusion properties and flow structure. To achieve an in-depth understanding of these mechanisms, simulations have been conducted.

Section 3 presents the experimental part, including the experimental assembly, working conditions and experimental results. Section 5 through 7 presents the numerical part, including the numerical model, boundary conditions, geometry, mesh, results validation and velocity contours. Finally, section 8 serves as a conclusion for the paper.

2. PROBLEM STATEMENT

When reducing the energy requirements of the building, one problem that arises is the proper spatial distribution of the low flow rates of fresh air to be injected in the living areas. If this problem is not effectively solved, it can result in a strong degradation of air quality and comfort due to inadequate mixing of the injected air with the room air. Dimotakis (2000) highlights that the generation and transition of turbulence are strongly influenced by the flow's geometry and initial perturbations, which are closely interconnected with the

Table 1 Measurement tools and sensors

Measurement tools and sensors	Model and accuracy
Multi-parameter ventilation meter	TSI-VelociCalc®Plus 8386-M-GB has a reading accuracy within ±3%.
Multi-thermometer	DKP300MA Key Pad Thermometer with alarm has a reading accuracy within ±3%.±0.1˚C.

mixing process. Many factors, such as humidity, latent heat, velocity, temperature, etc., can affect the comfort of the occupants. To ensure the comfort of the occupants, it is essential that the atmosphere of a living space is homogeneous in terms of supply velocity and temperature, which cannot be achieved by conventional terminal units alone. This requires appropriate air diffusers. The swirl jet concept is a newly proposed ventilation strategy for use in buildings, exposed stadiums in warm climates, and industrial offices. The present work concerns the dynamic behavior of jet from swirling diffusers, applied to improve air diffusion efficiency in the occupied zone to ensure thermal comfort. The main goal of this work is to improve the understanding of complex HVAC systems and provide insights that can be used to make informed decisions about how to design air diffusers. This will improve the air diffusion effectiveness in the occupied zone at a lower cost.

3. EXPERIMENTAL SET-UP

The main goal of this experimental setup is to improve air diffusion in occupied areas by using a new design of the HVAC system's diffusers. The experimental measurements were performed in a room with a height of 2.5 m, a length of 3.0 m, and a width of 2.5 m. Tests can be conducted under unfavorable pressure forces and vertical free jet conditions using these dimensions (Liu et al., 2017).

The current study focuses on the free jet rather than the confined jet. So, the effect of the walls in this room with these dimensions is almost negligible because they are far enough away to not influence the flow configuration. The experimental setup comprises of a chassis that supports the blowing mechanism (Fig. 1). The blowing mechanism comprises an air diffuser that directs air downwards. A multi-parameter ventilation meter is used to measure the flow velocities. To cover the maximum space, the probe is vertically and horizontally supported by a stem. Figure 1 depicts the experimental equipment used for free-mode measurements.

The swirling diffuser utilized in this investigation is schematically presented in Fig 2. Unlike the swirling diffusers studied in previous research (Hu 2003; Sajadi et al., 2011; Aziz et al., 2012; Raftery et al., 2015; Yau et al,. 2018), the present study uses a swirling diffuser with eleven aluminum fins mounted on a support

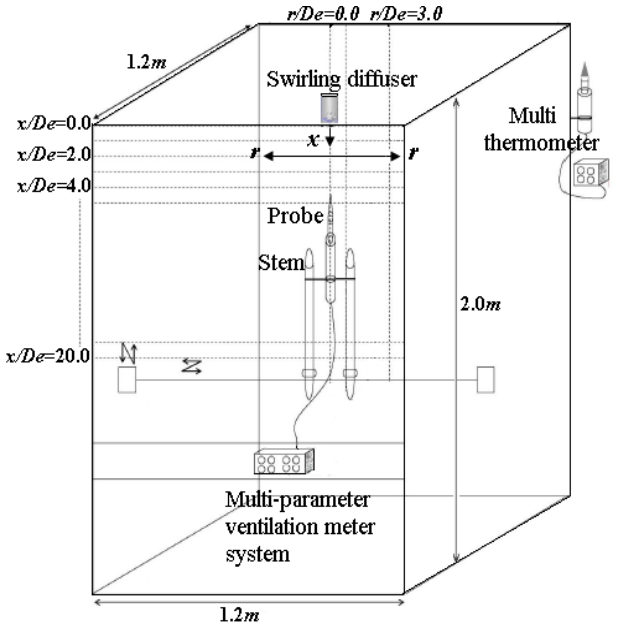

Fig. 1. Experimental installation description.

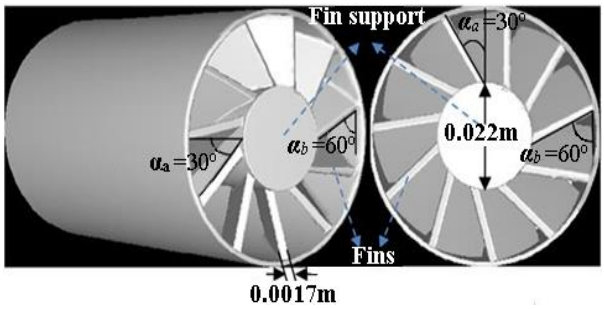

Fig. 2. Schematic description of the swirling diffuser.

with a diameter of 0.022 m (as shown in Fig. 2). To create a swirling motion, the fins are positioned at an inclination angles α_b of 60º and α_a of 30º relative to the blow plane and the axis of the jet, respectively. The fins are positioned such that they are attached to a stationary support (support fins), which leads to the formation of a recirculation zone behind them.

4. EXPERIMENTAL RESULTS

This experimental section presents the reduced velocities, U_r, obtained by calculating the ratio between the velocity at various points of the jet (U_i) and the velocity at the outlet of the diffuser (U_0). The radial and axial distances are expressed in dimensionless form as r/D_e ranging from 0 to 4.5 and x/D_e ranging from 1 to 20.

4.1. Experimental Profile of the Axial Velocity of a Swirling Jet

The U_r profile of a swirl jet is shown in Fig. 3 below.

Figure 3 illustrates the reduced velocity (U_r) in the axial direction over 20 D_e for a single swirling air jet. The axial velocity profile presents a Gaussian-like curve

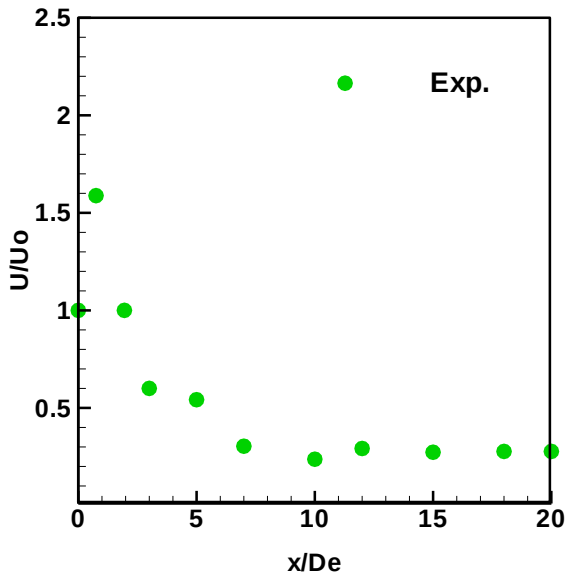

Fig. 3. Profile of the axial velocity from swirling air jet.

throughout the jet and highlights the velocity stability that appears when moving away from the diffuser's exit.

Between the axial stations x/D_e=0 and x/D_e=1, the equation of the line segment is y = 0.5881x + 1, and the slope of the line segment is 0.5881. So, there is a noticeable increase in velocity, reaching its maximum near the point x/D_e=1. This surge in velocity is attributed to the air generator's design, where the fins are attached to a fin support (as shown in Fig. 2), creating a recirculation region whose length depends on the equivalent diameter of the diffuser. Between the axial stations x/D_e=1 and x/D_e=3, the equation of the line segment is y = -0.49405x + 2.08215, and the slope is -0.49405. Therefore, the axial velocity undergoes a very rapid decrease down to 5 D_e from the point of flow initiation. For the station x/D_e=3 and x/D_e=5, the equation of the line segment is y = -0.029x + 0.687, and the slope of the line segment is -0.029. There is therefore a second slope which is less severe than the first one, reducing the velocity to almost 50% of its initial value. Then, the axial velocity experiences a very rapid decrease down to 10 D_e from the axis of jet, reaching almost 20% of its initial value. The rapid decrease in axial velocity leads to a transfer of kinetic energy towards the radial direction. Beyond x/D_e=10 up to x/D_e =20, the equation of the line segment is y = 0.0035x - 0.0115, and its slope value is 0.0035. In this region, the velocity intensity weakens and stabilizes along the flow.

Since the support for the fins is a solid cylinder rather than a hollow one, the air outlet will inevitably be on either side of it through the fins. When a fin is placed at an angle to the incoming jet, the velocity is influenced by the presence of the inclined fin wall. Therefore, the reduced velocities U_r increases in the axial direction as one moves away from centre of the fins support until it reaches its maximum at x/D_e =1. This region is known as the potential core, and it is a region in swirling jet where the air is relatively calm. The potential core is located near the centre of the fins support. The potential core is an important feature of the swirling jet. Therefore, the upsurge in velocity between x/D_e =0 and x/D_e =1 is attributable to the diffuser's design. In the transition zone (between x/D_e =1 to x/D_e =8), there is a significant decrease in velocity, which is explained by an expansion of the jet in the radial direction, due to the fins' inclination. Beyond the region of fully established flow ($x/D_e \geq 8$), the intensity of the velocity decreases and begins to stabilize, as the jet in this region is fully developed and unaffected by the fins.

From this, it can be deduced that the jet widens in the radial direction, since the inclination of the fins causes strong turbulence at the origin of the jet. Turbulent flow fields were induced by the diffuser fins. This result makes it possible to quantify the importance of the fins' inclination. It is also noticed that this type of jet significantly improves the homogenization of the flow.

4.2. Experimental Profiles of the Radial Velocities of a Swirling Air Jet

The velocity measurements in the radial directions were carried out for different stations.

First, the measurements taken for this jet configuration were made over the entire jet domain. The results obtained show that the flow is axisymmetric and indicates an equal transfer capacity in all radial directions. In the symmetrical plane (Fig. 4), it has been noticed:

- For the station x/D_e=3, and between the position r/D_e=0 up to r/D_e=0.5, there is an increase in velocity. As shown in Fig. 2, the fins support is a solid cylinder, not a hollow one, so the air outlet will be on its sides through the fins. Thus, the air velocity increases in the radial direction as one moves away from the jet center and/or the fins support, so that its maximum is near to the point r/D_e =0.5. Consequently, this increase in velocity is due to the geometric shape of the swirl diffuser (fin support). When one moves away from the point r/D_e= 0.5, it can be noticeable that the velocity decreases. This reduction in radial velocity is significant between the point r/D_e=0.5 and r/D_e =1. Beyond r/D_e=1 up to r/D_e =1.25, the velocity decreases linearly. At the station r/D_e=1.25 and 1.75, a second, less prominent slope than the first is perceived. Then the velocity undergoes a rapid decrease of up to $2D_e$ from the flow axis, reaching approximately 10% of its initial value.

- At the position r/D_e = 0.25 and the station x/D_e = 5, the velocity value is approximately the same as the value at the point r/D_e = 0. Starting from r/D_e=0.25, the velocity increases remarkably to reach the maximum near r/D_e=1. This increase in velocity is always due to the specific design of the swirling diffuser. Beyond r/D_e=1 up to r/D_e=1.5, the radial velocity rapidly begins to decrease, reaching almost 36% of its initial value. A second velocity slope is observed between r/D_e=1.5 and r/D_e=2, but it is less severe than the first one. The velocity stabilizes in this region and reaches its minimum value (almost 15% of its initial value).

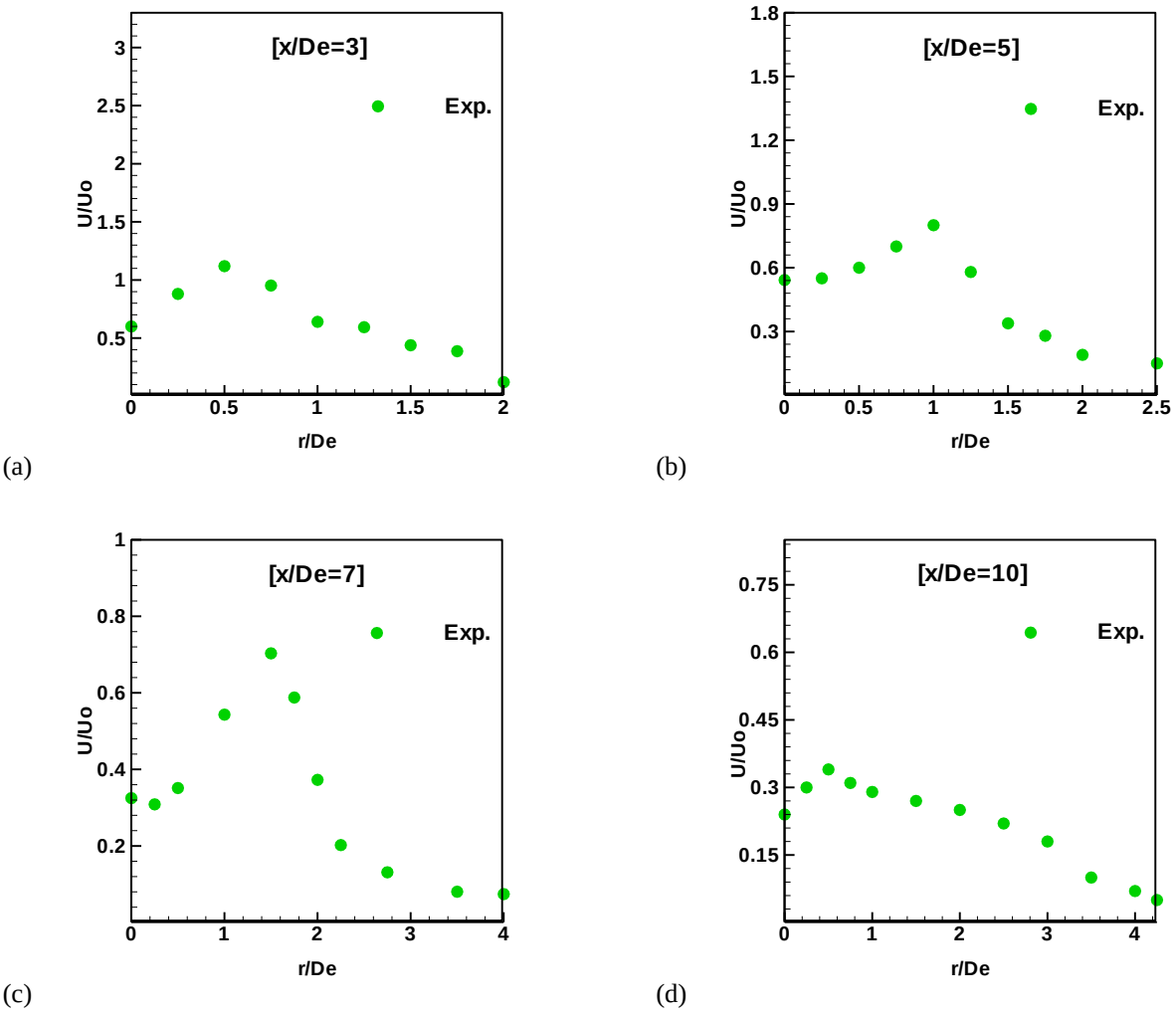

Fig. 4. Profiles of the radial velocity from swirling air jet at (a) x/D_e = 3, (b) x/D_e =5, (c) x/D_e =7, and (d) x/D_e =10 positions.

For station x / D_e =7, the velocity value is almost constant in the interval [0-0.25]. Then, it increases rapidly to a maximum value (70% of its initial value) close to r/D_e = 1.50. The periphery of the blow orifice has a greater velocity than its center, which is why the velocity at the jet center was low. This increase in velocity is attributable to the diffuser's design. Just after the point r/D_e=1.50, the velocity decreases rapidly and significantly until r/D_e=2.3, which is justified by the absence of the laminar cone. Beyond r/D_e=2.3 up to r/D_e=3.5, a decrease in velocity was also observed, but less accentuated compared to the decrease in the interval [1.5-2.3]. From r/D_e=3.5, the intensity of the velocity weakens and becomes regular along the flow, to reach its minimum value, almost 6% of its initial value.

- For station x/D_e=10, the velocity increases rapidly between the point x/D_e= 0 and 0.5 to reach its maximum value (36% of its initial value). Then, it begins to decrease gradually until at r/D_e = 3. From position r/D_e= 3 to r/D_e= 3.5, the velocity is reduced. Its stability begins just after the point r/D_e=3.5 and it takes a minimum value of 4% of its initial value.

According to the shape of the diffuser shown in Figure 2, the air outlet will be on the sides of the fin support through the fins. Therefore, the reduced velocities U_r increases in the radial direction as one move away from the jet center until it reaches its peak near the circumference of the fins, and then begins to decrease as one moves away from the fins, whether in the radial direction or axial direction. The radial outward expansion of the jet is due to the inclined fin wall effect. The velocity drop in the axial direction is physically understandable, which translates into a transfer of kinetic energy in a radial direction as shown by the radial velocity profiles (see Fig. 4). The decrease in velocity in the radial direction is caused by the jet mixing with the surrounding environment. The findings from examining the velocity profiles indicate that both the type of jet and the design of the diffuser exert a significant influence on the quality of the airflow mixture. The swirl jet ensures a relatively regular profile, resulting in a significant homogenization of the air in the living room and implying an improvement in the desertification of the airflow. It is noteworthy to state that the swirling jet ensures a superior expansion of the radial velocities compared to the circular jet. Therefore, due to its developmental advantage, the swirling jet would be more suitable for cooling or heating large spaces. The results of this research provide a good understanding of how the

diffuser's geometry affects the airflow pattern and can help in improving the design of diffusers.

5. NUMERICAL SIMULATION

In the CFD field, LES is a space filtering technique that involves computing the turbulent structures at the larger scales that are accountable for the exchange of momentum and energy in a fluid flow. A filter function is utilized in LES to differentiate between the large and small scales. This comprehensive approach allows for a good understanding of the complex behavior of fluid flow and enables accurate predictions of real-world phenomena. (Jones & Clarke 2008).

5.1. Filtered Navier-Stokes Equations

The incompressible filtered continuity equation, as proposed by Leonard (1975), is:

$$\frac{\partial}{\partial x_i}(\overline{u}_i) = 0 \tag{1}$$

And the filtered Navier–Stokes equations is:

$$\frac{\partial}{\partial x_i}(\overline{u}_i) + \frac{\partial}{\partial x_j}(\overline{u}_i\overline{u}_j) = -\frac{1}{\rho}\frac{\partial \bar{p}}{\partial x_i} + 2\nu\frac{\partial}{\partial x_j}\bar{S}_{ij} - \frac{\partial \tau_{ij}}{\partial x_j} \tag{2}$$

Leonard (1975) proposed a decomposition of the stress tensor as follows: $\tau_{ij} = R_{ij} + L_{ij} + C_{ij}$, with τ_{ij} gathering all the unclosed terms. Each term has a physical explanation, where R_{ij} presents the interactions between the sub-filter scales (SFS), L_{ij} presents the interactions between the large scales, and C_{ij} presents the cross-scale interactions between the small and large scales.

Filtered energy equation in LES can be expressed as:

$$\frac{\partial \rho\bar{h}_s}{\partial t} + \frac{\partial \rho\,\overline{u}_i\bar{h}_s}{\partial x_i} - \frac{\partial \bar{p}}{\partial t} - \overline{u}_j\frac{\partial \bar{p}}{\partial x_i} - \frac{\partial}{\partial x_i}\left(\lambda\frac{\partial \bar{T}}{\partial x_i}\right) = -\frac{\partial}{\partial x_j}\left[\underbrace{\rho(\overline{u_i h_s} - \overline{u}_i\bar{h}_s}_{Subgrid\ enthalpy\ flux}\right] \tag{3}$$

5.2. Subgrid-Scale Models

Because the subgrid-scale stress caused by the filtering operation is not known, it is crucial to model it. The Boussinesq hypothesis is utilized by the subgrid-scale models (Clark et al,. 1979), where the subgrid-scale turbulent stresses is modeled as:

$$\tau_{ij} - \frac{1}{3}\tau_{kk}\delta_{ij} = -2\mu_t\,\overline{S}_{ij} \tag{4}$$

The filtered term of static pressure includes the isotropic part of τ_{kk}, which is not modeled.

The $\bar{S}_{ij}$ obtained for the resolved scale through:

$$\overline{S}_{ij} \equiv \frac{1}{2}\left(\frac{\partial \overline{u}_i}{\partial x_j} + \frac{\partial \overline{u}_j}{\partial x_i}\right) \tag{5}$$

$$\tau_{ij} - \frac{1}{3}\tau_{kk}\delta_{ij} = 2\,\mu_t\left(S_{ij} - \frac{1}{3}S_{kk}\delta_{ij}\right) \tag{6}$$

For incompressible flows, it is possible to either include or disregard the term associated with τ_{kk} when adding it to the filtered pressure (Huang & Yang 2009).

5.2.1. Smagorinsky-Lilly Model

This model, initially suggested by Smagorinsky (1963), incorporates eddy viscosity, which is modeled through:

$$\mu_t = \rho L_s^2\sqrt{2\,\overline{S}_{ij}\bar{S}_{ij}} \tag{7}$$

With L_s is calculated using:

$$L_s = min\,(\kappa d, C_s\Delta) \tag{8}$$

There Δ is determined by:

$$\Delta = V^{1/3} \tag{9}$$

5.2.2. Wall-Adapting Local Eddy-Viscosity (WALEVM) Model

The WALEVM model (Kim, 2004) employs a method of modeling eddy viscosity, which can be expressed as:

$$\mu_t = \rho L_s^2\frac{\left(S_{ij}^d S_{ij}^d\right)^{3/2}}{\left(\bar{S}_{ij}\bar{S}_{ij}\right)^{5/2} + \left(S_{ij}^d S_{ij}^d\right)^{5/4}} \tag{10}$$

In the WALEVM model, the definitions of S_{ij}^d and L_s are as follows:

$$L_s = min\left(\kappa d, C_w V^{1/3}\right) \tag{11}$$

$$S_{ij}^d = \frac{1}{2}\left(\bar{g}_{ij}^2 + \bar{g}_{ji}^2\right) - \frac{1}{3}\delta_{ij}\bar{g}_{kk}^2\,,\bar{g}_{ij} = \frac{\partial \overline{u}_i}{\partial x_j} \tag{12}$$

In ANSYS Fluent, the WALEVM constant, C_w, has a default value of 0.325, which has been shown to provide adequate results for a large variety of flows. The remaining parts of the notation are identical to those used in the LES/S-LM.

5.2.3. Dynamic Kinetic Energy Subgrid-Scale Model

This model reproduces the model suggested by Kim and Menon (1997). The k_{sgs} is computed using the following formula:

$$k_{sgs} = \frac{1}{2}\left(\overline{u_k^2} - \overline{u}_k^2\right) \tag{13}$$

Where μ_t is calculated using k_{sgs} as:

$$\mu_t = C_k\,k_{sgs}^{1/2}\,\Delta\,f \tag{14}$$

With Δ_f is the filter-size defined as: $\Delta_f \equiv V^{1/3}$.

The subgrid scale stress expressed as:

$$\tau_{ij} - \frac{2}{3}\,k_{sgs}\delta_{ij} = -2C_k\,k_{sgs}^{1/2}\,\Delta\,f\bar{S}_{ij} \tag{15}$$

By resolving the transport equation, k_{sgs} is obtained.

$$\rho\frac{\partial \bar{k}_{sgs}}{\partial t} + \frac{\partial \overline{u}_j\bar{k}_{sgs}}{\partial x_j} = -\,\tau_{ij}\frac{\partial \overline{u}_i}{\partial x_j} - C_\varepsilon\frac{k_{sgs}^{3/2}}{\Delta_f} + \frac{\partial}{\partial x_j}\left(\frac{\mu_t}{\sigma_k}\frac{\partial k_{sgs}}{\partial x_j}\right) \tag{17}$$

σ_k is hardwired to 1.0. Kim (2004) offers a thorough explanation of how the model was implemented and validated in ANSYS Fluent.

6. Boundary Conditions

The figure below shows the boundary conditions for the case under study. The dimensions of the room are much greater than those of the air diffusion zone.

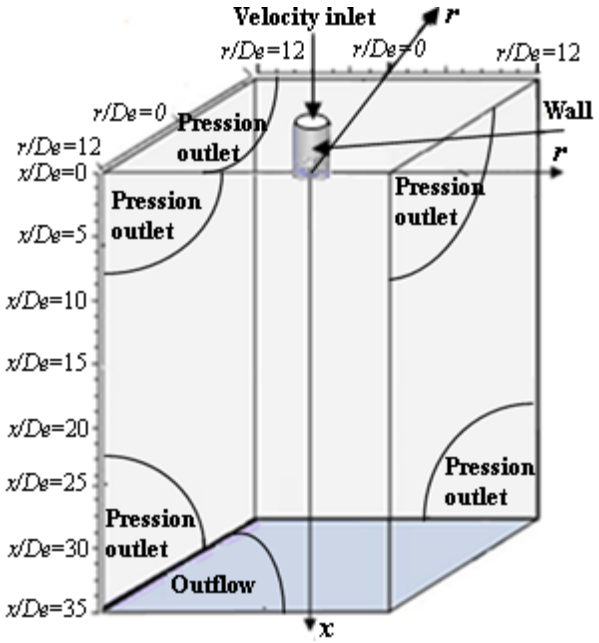

Fig. 5. Schematic of Boundary Conditions.

The initial conditions for the turbulence models (LES/K-ETM, LES/WALEVM, and the LES/S-LM) are:

- Inlet velocity: 7.7 (m/s);
- Turbulence intensity: 5 (%);
- Inlet temperature: 223.3(K);
- Reynolds Number: $R_{eynolds}$ =3.00*10^5.

6.1. Grid Study

The computational domain for this investigation is presented in Fig. 6. For this three-dimensional study, the software used to obtain the simulation results was ANSYS Fluent 2021 R2 (OpenMP). Due to the complexity of the geometry, an unstructured tetrahedral mesh primarily composed the computing grid.

In this study several parameters were considered to evaluate accuracy and reliability of the mesh. Notably, the smallest distance from the wall was found to be 2.23*10e-4 m, which proved sufficient to accurately capture near-wall flow features and turbulence effects. Moreover, the study explored the minimum and maximum values of orthogonality, which were found to be 0.4 and 0.97, respectively. To ensure numerical stability, the maximum value of skewness was determined to be 0.95. The aspect ratios were also

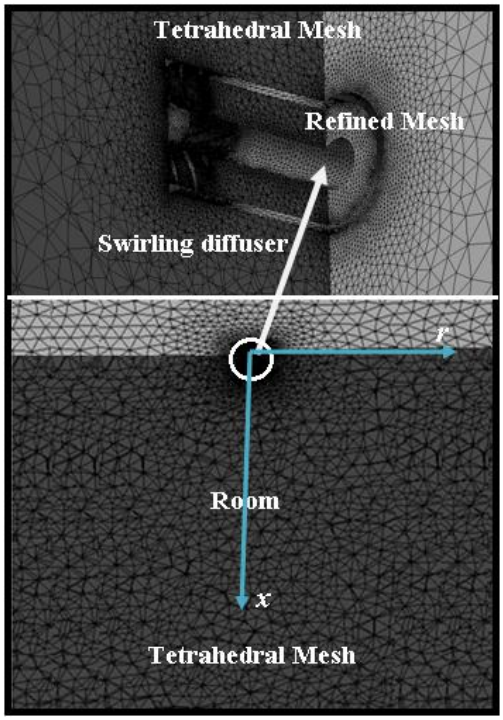

Fig. 6. Meshing of the calculation domain.

considered, with the minimum and maximum values being 1:3. Overall, these details are crucial for evaluating the accuracy and reliability of the tetrahedral unstructured mesh used in the study.

In the case of the swirling jet, three different meshes were tested to evaluate their impact using the LES/K-ETM turbulence model.

Table 2 shows that the numerical uncertainty of the fine-grid solution for the average velocity of air in the axial direction is 0.006%, indicating that the grid sizes used for the simulation are appropriate. However, based on the GCI equation mentioned by Celik et al (2008), it appears that the convergence is oscillatory, as the value of the GCI equation approaches 0.

Table 2 Numerical uncertainty of the fine-grid solution.

	Meshing-1 Coarse	Meshing-2 Medium	Meshing-3 Fine (Examined)
No of Elements, N	2718138	3393912	3752674
Mesh Refinement Ratio, r	-	1.075	1.033
Average Velocity of Air, Axial Direction	0.639	0.659	0.660
Relative Error, δ	-	0.030	0.001
Order of convergence, p	-	41.5	93.4
GCI	-	0.0019	6.33232e-5
GCI%	-	1.9%	0.006%

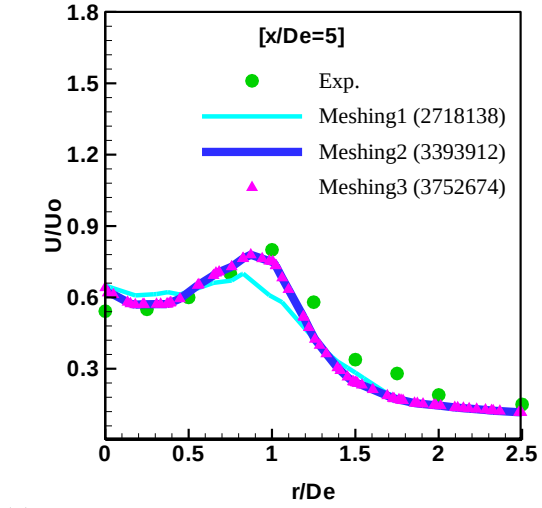

(a)

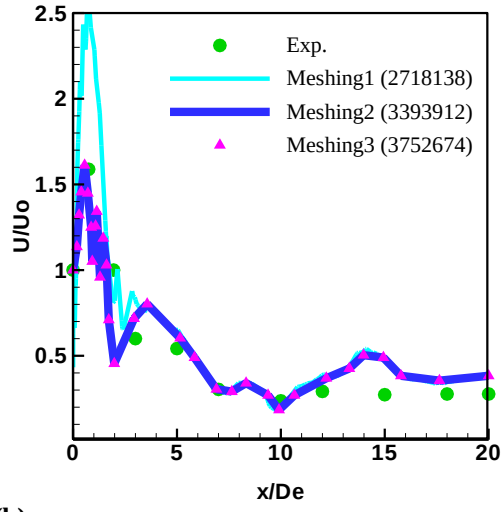

(b)

Fig. 7. Mesh effect for the (a) radial and (b) axial velocity with the LES/K-ETM.

From Fig. 7 and Table 2, it is clear that mesh 3 is appropriate for this simulation. As a result, mesh 3 was selected for the remaining simulations.

7. NUMERICAL RESULTS AND VALIDATION

Achieving good agreement with experimental results is a crucial part of validating a simulation or model. When simulation results match experimental results, it indicates that the simulation or the model well approaches and/or reproduces the physics of flows being studied.

7.1. Axial Reduced Velocity Profiles for A Swirling Jet

At different stations, Figure 8 displays a comparison of the experimental and numerical findings for the velocity (U_r). Knowing that, the numerical results were acquired by testing three models: LES/SL, LES/ WALEV, and LES/K-ETM. Turbulence models are mathematical models that attempt to predict the behavior of turbulent flows. There are several different types of turbulence models, and each one has its own strengths and weaknesses. In fact, different turbulence models

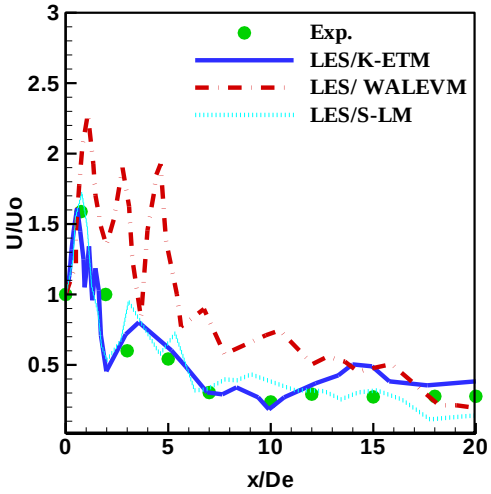

Fig. 8. Numerical and experimental velocity profiles in the axial direction.

have different levels of accuracy depending on the application and the specific conditions being modelled.

The models used in the simulation should be validated against experimental data to ensure that they represent well the physics of the system being reproduced. This can involve comparing simulation results to experimental data obtained from the same system under similar conditions.

Overall, the velocity predicted by a turbulence model is highly dependent on the specific model used, as well as the geometry and boundary conditions of the system being simulated. Validating turbulence models against experimental data is a crucial step to ensure that they predict well the behavior of real-world flows.

Figure 8 demonstrates that the velocities predicted by the LES/K-ETM and LES/S-LM models are consistent with those of the experiment. However, none of the turbulence models are able to accurately and simultaneously predict the axial variation of velocity (U_r) across the entire domain of the jet.The Root Mean Squared Error (RMSE) is a widely used measure to assess the precision of a turbulence model used for prediction purposes. Specifically, it measures the magnitude of the deviation between predicted and actual values of a target variable, typically in the context of a regression analysis. Lower values of RMSE indicate better turbulence model performance. It is important to carefully select the appropriate turbulence model and to validate the model predictions against experimental data.

After comparing the results derived from LES/SL, LES/WALEVM, and LES/K-ETM models with the experimental results along the axial direction, the root mean squared error has been calculated which is respectively as follows: 14.13%, 41.38% and 11.43%. The turbulence model LES/K-ETM is more accurate in predicting the behavior of this type of jet (swirling jet) than other turbulence models. On the other hand, the LES/S-LM and LES/WALEVM turbulence models are less accurate in predicting complex this swirling jet.

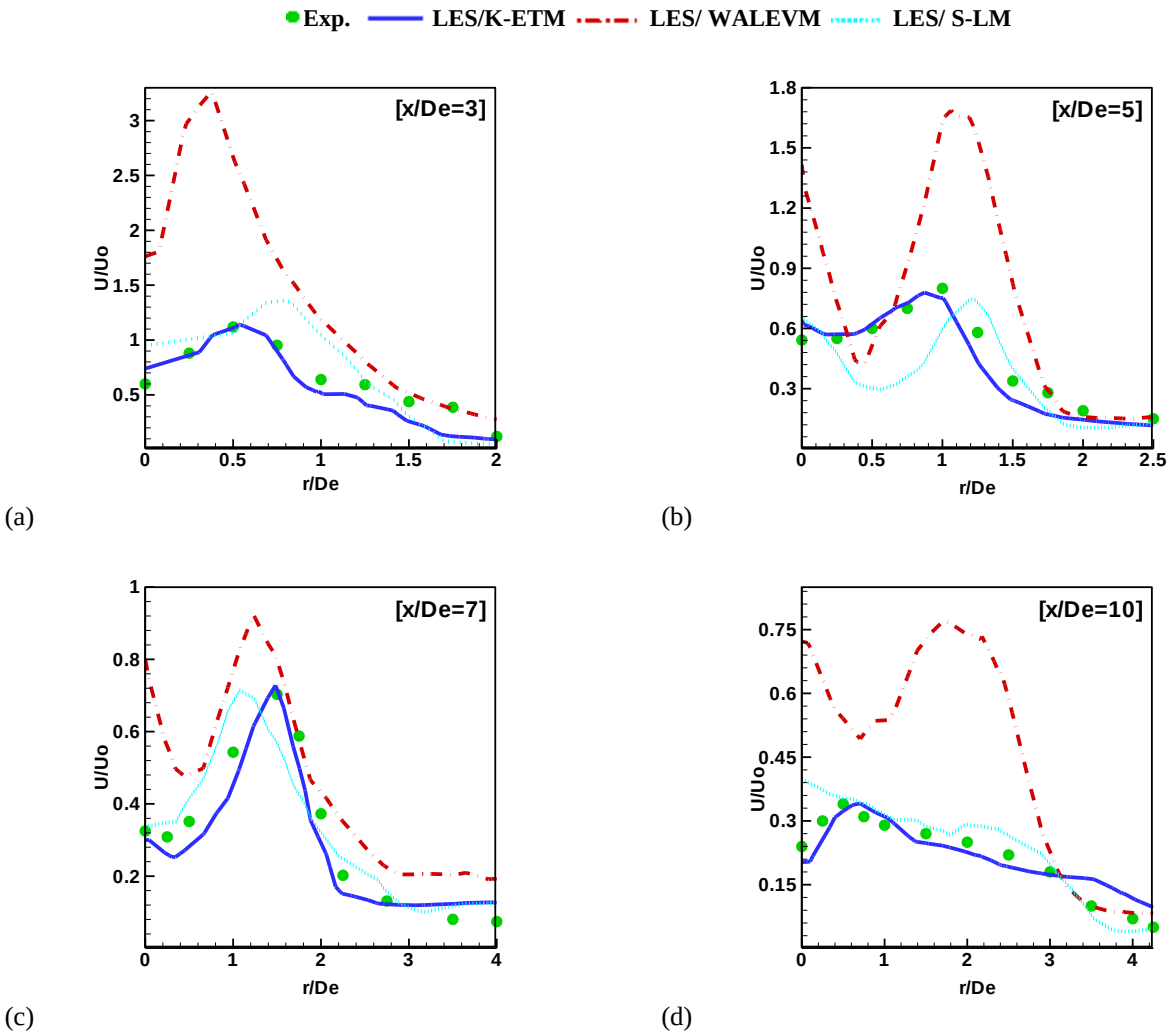

Fig. 9. Comparison of numerical and experimental velocity profiles at (a) x/D_e = 3, (b) x/D_e =5, (c) x/D_e =7, and (d) x/D_e =10 in the radial direction.

As shown in Fig. 8, the dimensionless axial velocities predicted by the LES/K-ETM are satisfyingly consistent with the experimental data. Therefore, it can be concluded that the predictions are validated correctly.

7.2. Reduced Radial Velocity Profiles for A Swirling Jet

The radial velocity profiles predicted by a turbulence model depend on the specific model used, the geometry of the system being simulated, and the boundary conditions applied.

Turbulence models are used to predict the turbulent flow behavior, which are characterized by chaotic fluctuations and vortices that are difficult to predict using traditional fluid dynamics equations. The following Figure illustrates the radial velocity profiles predicted by three turbulence models, compared with measurements of experimental at the various stations. The LES/S-LM model gives a similar shape to the experimental values, but with some deviation. The LES/WALEVM turbulence model predicts unsatisfactory evolutions of the dynamic quantities.

Moreover, not all turbulence models can predict the radial velocity evolution in the entire flow domain simultaneously. The predicted velocities by the LES/K-ETM are considered as appropriately validated. After comparing the results obtained using the LES/S-LM, LES/WALEVM and LES/K-ETM with the experimental data in the radial directions, the root mean squared error has been calculated and is shown in Table 3.

Table 3 Mean square error in the radial direction

	LES K-ETM	LES S-LM	LES WALEVM
X/D_e=3	10.85%	19.09%	82.02%
X/D_e=5	6.06 %	13.34%	35.79%
X/D_e=7	4.72%	6.84%	22.97%
X/D_e=10	2.94%	3.70%	23.33%
Total RMSE	6.14%	10.74%	41.02%

The superior performance of the LES/K-ETM turbulence model in predicting the behavior of this jet, as indicated by its lower RMSE values, is further confirmed by the correctly validated velocities predicted by the model, as shown in Table 3.

The numerical results (Figs. 8 and 9) show that the axial velocities predicted by the LES/S-LM and LES/K-

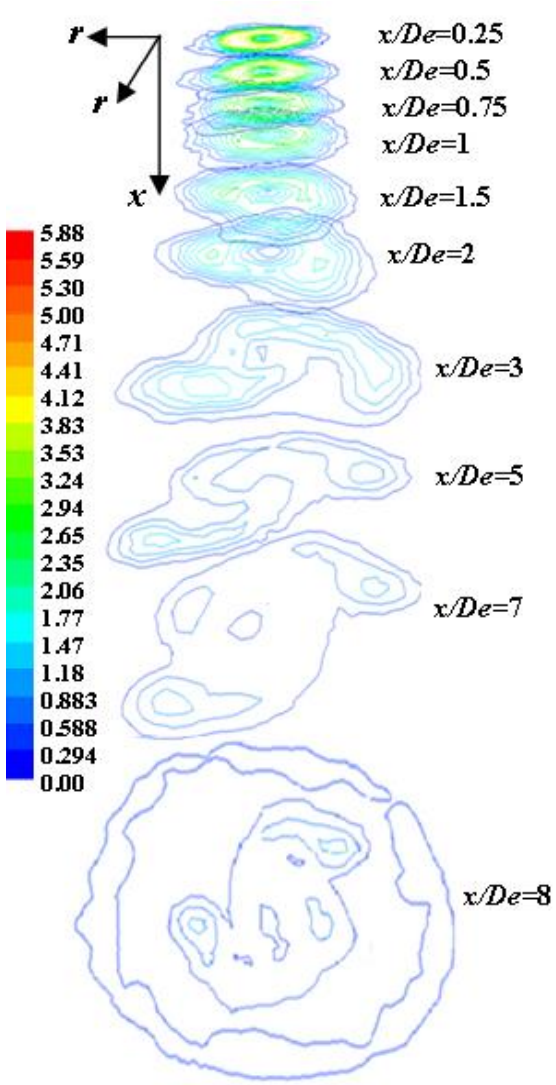

Fig. 10 Velocity contours at different positions of a swirling jet.

ETM are generally in satisfactory consistent with the experimental results. However, it is only the LES/K-ETM model gives results close to those obtained from the experiment and satisfactorily predicts the evolution of velocities in both directions of the jet. This is confirmed by the lower root mean squared error values of this model compared to the others in both radial and axial directions.

The specific results obtained from this simulation depend on a wide range of factors, including the accuracy of the model used, the quality of the meshes, and the assumptions made in the simulation, etc.

7.3. Velocity Contours

The goal of presenting the velocity contours is to test the effectiveness of new diffuser design in improving the performance of HVAC systems, as well as to analyze and understand their behavior.

The turbulence model LES/K-ETM is used to simulate how this swirling jet would perform, and to make predictions about its behavior and/or performance. With the turbulence model LES/K-ETM, ANSYS-FLUENT enables the visualization of velocity contours at various axial stations (x/D_e=0.25, 0.50, 0.75, 1, 1.50, 2, 3, 5, 7 and 8).

Figure 10 shows the dynamic behavior of the swirling jet at different axial and radial distances. Upon analysis of Fig. 10, it is noted that the radial and axial velocities near the blowing orifice are non-uniform, but they become more homogeneous after a certain distance from the blowing orifice of the diffuser, both radially and axially.

From this perspective, it can be concluded that the fins play a crucial role in enabling the relative spreading of the jet, particularly before the potential core region and the transition region (x/D_e <8). As the fully developed region is reached ($x/D_e \geq 8$), the influence of the fins diminishes, resulting in the swirling jet taking a circular shape similar to that of a circular jet.

The behavior of the jet, as present in Fig. 10, confirms that the swirling jet expands more in the radial direction compared to a non-swirl or circular jet without fins. It is also observed that the fins' walls modify the shape of the jet, causing it to spread and generate a recirculation zone behind the fin support. This recirculation zone causes the vortex to unwind before decomposing against the fin surface.

When inclined fins are placed in a diffuser, they have a significant impact on the jet. The inclined fins alter the flow field around the jet by creating vortices and changing the direction of the jet, which increases its expansion in the radial direction. Since the fins support a solid cylinder and not a hollow one (see Fig. 2), the air outlet will be on its sides through the fins. Therefore, the air velocity increases in the radial direction as one moves away from the center of the fins support until it reaches its peak near the circumference of the fins, and then begins to decrease as one moves away from the fins, whether in the radial direction or axial direction.

In the region of the potential core (from x/D_e=0.25 to x/D_e=1), the expansion of the jet in the radial direction is somewhat weak. In contrast, in the transition zone (between x/D_e=1 and x/D_e= 7), a significant expansion of the jet in the radial direction is observed due to the inclination of the fins. Beyond the fully established flow region ($x/D \geq 8$), the jet is fully developed and appears unaffected by the fins, taking on a circular shape.

The fins inclination causes strong turbulence at the origin of the jet. It can be clearly seen that the presence of fins has a significant impact on the diffuser's performance, and it can be confirmed that these fins have a great impact on enhancing the induction effect of the diffuser.

Simulation results are obtained to gain insight into complex systems, processes, and phenomena that are difficult to study through direct observation or experimentation. They can be utilized to improve diffuser designs and test the performance of the jets originating from them. In general, these simulation results can provide valuable insights into heating,

ventilation, and air conditioning systems (HVAC) by analyzing the complex phenomena related to them. They can help researchers and practitioners make more informed decisions with the aim of improving and developing these systems at the lowest cost.

8. CONCLUSION

The dynamics of a swirling jet generated by inclined fins has been studied experimentally and numerically. This type of jet is applied to improve the comfort of residential rooms by enhancing the diffusion of air in the occupied zone at a lower cost. This study and its results help to deepen the comprehension of swirling diffuser airflows and the effect of geometric characteristics of the diffuser on their performance.

According to the analysis of experimental and numerical results, it has been found that the mixing performance of the airflow is dependent on the geometric shape of the diffuser. Therefore, optimizing parameters such as the diffuser's geometry, significantly improve the efficiency of air diffusion and homogenization with the ambient air. The swirling diffuser is characterized by a large central recirculation zone, and inside this zone, the current lines move radially to widen the distribution of the air along the jet axis. The turbulent jets are of significant practical importance in the application of air conditioning and cooling systems. The imposition of swirling jets promotes mixing processes as well as mass and heat transfer. Thus, the use of this type of diffuser ensures a greater improvement in the homogeneity of the air in the treated area. This is because the homogenization of the air in the radial direction is linked to the greater expansion of the jet, which is well ensured by this type of swirling jet. The swirling jet therefore has certain advantages for the homogenization of the ambient treated by mixing, since it provides an interesting combination of the movement of the free jet and the rotational movement of the fluid. It expands more quickly than an axisymmetric free jet while allowing better air distribution in the premises, thus ensuring appreciable comfort conditions.

Predicting the velocity field inside air-conditioned rooms remains a challenging task, especially in the case of large rooms. To improve the predictions of the turbulence models and to determine the most adequate model for this type of flow, three models were tested: the LES/WALEVM, LES/S-LM, and the LES/K-ETM.

The three models could not simultaneously predict the dynamic evolution of the flow in all directions of the jet domain. The LES/K-ETM model gave results close to those obtained experimentally and satisfactorily predicted the evolution of velocities in all directions of the jet domain, whether in the axial direction or in the radial directions of the jet. The swirl jet ensures homogenization with a large spread, which makes it possible to treat a large space. The characterizations of this diffuser's design appear important for its application to HVAC systems.

CONFLICT OF INTERESTS

The authors declare that they have no known competing financial interests or personal relationships that could have appeared to influence the work reported in this paper.

AUTHORS' CONTRIBUTIONS

Bennia A: Conceived and designed the numerical study, contributed to the experimental design, performed laboratory experiments conducted data analysis, and wrote the manuscript; Reffas, M: Assisted in data interpretation; A. H. Khan: Critically reviewed the manuscript; H. E. Mohamadi: Reviewed the manuscript; M. Lateb: Reviewed the manuscript; H. Fellouah: Provided guidance and expertise, reviewed and revised the manuscript.

REFERENCES

Awbi, H. B. (1989). Application of computational fluid dynamics in room ventilation. *Building and Environment*, 24(1), 73-84. https://doi.org/10.1016/0360-1323(89)90018-8

Aziz, M, A., Gad, I. A. M., El Shahat, F. A., & Mohammed, R. H. (2012). Experimental and numerical study of influence of air ceiling diffusers on room air flow characteristics. *Energy and Buildings*, 55, 738-746. https://doi.org/10.1016/j.enbuild.2012.09.027

Bennia, A., H. Fellouah, A. Khelil, L. Loukarfi and H. Naji (2020). Experiments and large-eddy simulations of lobed and swirling turbulent thermal jets for HVAC's applications. *Journal of Applied Fluid Mechanics* 13(1), 103-117. https://doi.org/10.29252/jafm.13.01.29970

Bennia, A., Loukarfi, L., Khelil, A., Mohamadi, S., Braikia, M., & Naji, H. (2018). Experimental and numerical investigation of a turbulent lobed diffuser jet: Application to residential comfort. *Mechanics & Industry*, 19(1), 104. https://doi.org/10.1051/meca/2016078

Bennia, A., Loukarfi, L., Khelil, A., Mohamadi, S., Braikia, M., & Naji, H. (2016). Contribution to the experimental and numerical dynamic study of a turbulent jet issued from lobed diffuser. *Journal of Applied Fluid Mechanics*, 9(6), 2957-2967. https://doi.org/10.29252/jafm.09.06.25953

Bennia, A., Loukarfi, L., Braikia, M., Khelil, A., & Naji, H. (2015). Etude expérimentale d'un jet turbulent à diffuseur muni de lobes: Application au confort dans les locaux à usage d'habitation. *Nature & Technology*, (13), 54.

Celik, I. B., Ghia, U., Roache, P. J., Freitas, C. J., Coleman, H., & Raad, P. E. (2008). Procedure for estimation and reporting of uncertainty due to discretization in CFD applications. *Journal of Fluids*

Engineering, 130, 078001. https://doi.org/10.1115/1.2960953

Clark, R. A., Ferziger, J. H., & Reynolds, W. C. (1979). Evaluation of subgrid-scale models using an accurately simulated turbulent flow. *Journal of fluid mechanics*, 91(1), 1-16. https://doi.org/10.1017/S002211207900001X

Dimotakis, P. E. (2000). The mixing transition in turbulents flows. *Journal of Fluid Mechanics*, 409, 68-69. https://doi.org/10.1017/S0022112099007946

Hu, S. C. (2003). Airflow characteristics in the outlet region of a vortex room air diffuser. *Building and Environment*, 38(4), 553-561. https://doi.org/10.1016/S0360-1323(02)00187-7

Huang, Y., & Yang, V. (2009). Dynamics and stability of lean-premixed swirl-stabilized combustion. *Progress in Energy and Combustion Science*, 35(4), 293-364. https://doi.org/10.1016/j.pecs.2009.01.002

Huo, Y., Haghighat, F., Zhang, J. S., & Shaw, C. Y. (2000). A systematic approach to describe the air terminal device in CFD simulation for room air distribution analysis. *Building and Environment*, 35(6), 563-576. https://doi.org/10.1016/S0360-1323(99)00047-5

Jones, D. A., & Clarke, D. B. (2008). *Simulation of flow past a sphere using the fluent code*. Maritime Platforms Division DSTO Defence Science and Technology Organisation, 506 Lorimer St, Fishermans Bend, Victoria 3207 Australia.

Khan, M. A. H., Bennia, A., Lateb, M., & Fellouah, H. (2022). Numerical investigation of thermal comfort using the mixing and displacement ventilation systems within a fitting room. *International Journal of Heat and Mass Transfer*, 198, 123379. https://doi.org/10.1016/j.ijheatmasstransfer.2022.123379

Kim, S. E. (2004). Large eddy simulation using unstructured meshes and dynamic subgrid-scale turbulence models. *Proceedings of the 34th AIAA Fluid Dynamics Conference and Exhibit*, Portland, Oregon, 2004-2548. United States. https://doi.org/10.2514/6.2004-2548

Kim, W. W., & Menon, S. (1997). *Application of the localized dynamic subgrid-scale model to turbulent wall-bounded flows*. Proceedings of the 35th Aerospace Sciences Meeting and Exhibit, Reno, Nevada, 210. United States.

Koskela, H. (2004). Momentum source model for CFD-simulation of nozzle duct air diffuser. *Energy and Buildings*, 36(10), 1011-1020. https://doi.org/10.1016/j.enbuild.2004.06.013

Kumar, M., Chong, C. T., & Karmakar, S. (2022). Comparative assessment of combustion characteristics of limonene, Jet A-1 and blends in a swirl-stabilized combustor under the influence of pre-heated swirling air. *Fuel*, 316, 123350. https://doi.org/10.1016/j.fuel.2022.123350

Leonard, A. (1975). Energy cascade in large-eddy simulations of turbulent fluid flows. *Advances in geophysics*, 18, 237-248. https://doi.org/10.1016/S0065-2687(08)60464-1

Liu, M., Zhang, Y., & Pan, J. (2017). Experimental investigation of the aerodynamic characteristics of a high-speed train under crosswind conditions. *Journal of Wind Engineering and Industrial Aerodynamics*, 166, 22-32. https://doi.org/10.1016/j.jweia.2018.03.021

Luo, S., Heikkinen, J., & Roux, B. (2004). Simulation of air flow in the IEA Annex 20 test room—validation of a simplified model for the nozzle diffuser in isothermal test cases. *Building and Environment*, 39(12), 1403-1415 https://doi.org/10.1016/j.buildenv.2004.04.006

Nielsen, P. V. (1976). *Flow in air conditioned rooms.* [Doctorol thesis, the Technical University]. Denmark.

Nielsen, P. V. (1989). *Representation of boundary conditions at supply openings*. Dept. of Building Technology and Structural Engineering, Aalborg University. Gul Serie Vol. R8902 No. 4.

Nielsen, P. V. (1992). Description of supply openings in numerical models for room air distribution. *ASHRAE Transactions*, 98, 963–971. https://jglobal.jst.go.jp/en/detail?JGLOBAL_ID=200902017766811371

Nielsen, P. V. (1997). *The Box Method: A Practical Procedure for Introduction of an Air Terminal Device in CFD Calculation.* Dept. of Building Technology and Structural Engineering, Aalborg University. Gul serie Vol. R9744 No. 34.

Nielsen, P. V. (1998). *The Prescribed Velocity Method: A Practical Procedure for Introduction of an Air Terminal Device in CFD Calculation*. Dept. of Building Technology and Structural Engineering, Aalborg University. Gul serie Vol. R9827 No. 40.

Nielsen, P. V. (2015). Fifty years of CFD for room air distribution. *Building and Environment*, 91, 78-90. https://doi.org/10.1016/j.buildenv.2015.02.035

Raftery, P., Bauman, F., Schiavon, S., & Epp, T. (2015). Laboratory testing of a displacement ventilation diffuser for underfloor air distribution systems. *Energy and Buildings*, 108, 82-91. http://dx.doi.org/10.1016/j.enbuild.2015.09.005

Sajadi, B., Saidi, M. H., & Mohebbian, A. (2011). Numerical investigation of the swirling air diffuser: Parametric study and optimization. *Energy and Buildings*, 43(6), 1329-1333. https://doi.org/10.1016/j.enbuild.2011.01.018

Smagorinsky, J. (1963). General circulation experiments with the primitive equations: I. The basic experiment. *Monthly Weather Review*, 91(3), 99-164. https://doi.org/10.1175/1520-0493(1963)091<0099:GCEWTP>2.3.CO;2

Tavakoli, E., & Hosseini, R. (2013). Large eddy simulation of turbulent flow and mass transfer in far-field of swirl diffusers. *Energy and Buildings*, 59, 194-202. https://doi.org/10.1016/j.enbuild.2012.12.029

Villafruela, J. M., Castro, F., San José, J. F., & Saint-Martin, J. (2013). Comparison of air change efficiency, contaminant removal effectiveness and infection risk as IAQ indices in isolation rooms. *Energy and Buildings*, 57, 210-219. https://doi.org/10.1016/j.enbuild.2012.10.053

Wang, K., Xie, D., Cao, Q., Hu, J., Tang, Y., Shi, B., & Wang, N. (2022). Characteristics of oxy-methane flame in an axial/tangential swirl jet burner. *Experimental Thermal and Fluid Science*, 139, 110732. https://doi.org/10.1016/j.expthermflusci.2022.110732

Xie, D., Cao, Q., Tang, Y., Wang, K., Chen, X., Wang, N., & Shi, B. (2022). Ethanol spray tubular flame established in a swirling air flow. *Experimental Thermal and Fluid Science*, 134, 110616. https://doi.org/10.1016/j.expthermflusci.2022.110616

Yau, Y. H., Poh, K. S., & Badarudin, A. (2018). A numerical airflow pattern study of a floor swirl diffuser for UFAD system. *Energy and Buildings*, 158, 525-535. https://doi.org/10.1016/j.enbuild.2017.10.037

Zhao, B., Li, X., & Yan, Q. (2003). A simplified system for indoor airflow simulation. *Building and Environment*, 38(4), 543-552. https://doi.org/10.1016/S0360-1323(02)00182-8